Thermal radiation from two-dimensionally confined modes in microcavities

S. Maruyama and T. Kashiwa
Institute of Fluid Science, Tohoku University, Katahira, Aoba-ku, Sendai, 980-8577, Japan

H. Yugami[a)]
Graduate School of Engineering, Tohoku University, Aramaki, Aoba-ku, Sendai, 980-8579 Japan

M. Esashi
NICHe, Tohoku University, Aramaki, Aoba-ku, Sendai, 980-8579, Japan

(Received 12 March 2001; accepted for publication 3 July 2001)

A two-dimensional array of a microcavity with a high aspect ratio is made on a Cr-coated Si surface using the micromachining technology. The thermal emission spectra whose wavelength is close to the dimension of cavity aperture (5 μm) are measured on samples with a different aspect ratio. The clear selective emission bands corresponding to the two-dimensionally confined electromagnetic modes are demonstrated experimentally. It is found that the low emissivity of the base material is essential to obtain the high spectral selectivity of thermal radiation. The direction and polarization properties are also examined. The dominant peaks of the emission spectra can be explained by a simple cavity resonator model. © *2001 American Institute of Physics.* [DOI: 10.1063/1.1397759]

It is well known that properties of thermal radiation form a solid change according to the surface structure. Numerous studies have been reported for the relationship between the thermal radiation properties and macroscopic surface structure.[1,2] When the scale of the surface geometry is close to that of the thermal radiation wavelength, emission spectra show unique features by the electromagnetic interactions at the surface. Zemel *et al.* have reported about directional and polarized spectral emittance from one-dimensional Si lamellar gratings extensively.[3–5] They observed selective thermal emission by electromagnetic standing waves in microgrooves. Heinzel *et al.*[6] have reported the simulation study of selective emission from the tungsten surface with the periodic microstructures using the coupled wave theory. Recently, Sai *et al.* have reported thermal emission control by two-dimensional periodic surface structures made by Si anisotropic etching at the near infrared region.[7] As a practical application, Waymouth[8] suggested that the effects of the microcavities can be applied to the improvement of the efficiency of the incandescent lamp. This effect was called ''cavity quantum electrodynamics'' (CQE) by Haroche and Kleppner.[9] However, clear evidence of the CQE effect on thermal radiation from microcavity has not been reported by the following experiments, because it is difficult to fabricate deep microcavities with nanoscale periodicity.

In this letter, the thermal emission from two-dimensionally confined modes is clearly observed on a microcavity arrayed surface on which square cavities are densely located. The emittance of almost unity is obtained for deep microcavity with low base emittance. A preliminary analysis using the cavity resonator model is also performed.

A two-dimensional microcavity array is made on Si wafer surface using integrated-circuit fabrication technology. The computer aided design grating pattern is exposed on the resist coated wafer surface with electron beam lithography system. To make cavities with a high aspect ratio, deep etching is carried out with inductively-coupled-plasma reactive ion etching (ICP RIE) system. SF_6 and C_4F_8 gases are used for etching. In order to enhance the cavity effect, chromium that has high reflectivity in the infrared region is sputtered on the silicon wafer surface, because silicon is a transparent medium in the infrared region. The thickness of Cr (about 150 nm) is decided from the skin depth worked out using complex refractive indices of chromium.

The top and cross sectional view of sample images measured by scanning electron microscopy are shown in Fig. 1. The aperture width of a microcavity ($L_x = L_y$) discussed here is fixed to 5 μm, and the depth (L_z) is changed. The samples with different cavity depth are numbered for convenience as follows; No. I ($L_z = 2.0\,\mu$m), No. II (4.9 μm), No. III (7.3 μm), and No. IV (13.7 μm). The cavities are arrayed at intervals of 1 μm, and the total area of cavity array is $25 \times 25\,\text{mm}^2$. ICP RIE is a powerful tool to make deep cavities. However, due to the character of this etching process, asperity is observed on the cavity wall.

Measurements of emission spectra have been worked out in an isothermal room, where the temperature and humidity is kept at 297 K and less than 40%, respectively. Emission spectra from samples are measured by a Fourier transform infrared spectrophotometer, which is reformed to introduce the external emission light into the interferometer. The spectral resolution is set to 16 cm^{-1} and the Happ–Genzel function is used for apodization. Samples, a dummy black body and a reference flat sample, are heated isothermally in a radiation shielded vacuum container equipped with KRS-5 windows. The temperature at the sample surface, dummy black body furnace, and the inside of the heater is measured by thermocouples. A cone-shaped dummy black body is located beside the samples. The spectral intensities of the samples and the dummy black body have been measured simultaneously, and the emittance of samples has been derived from the comparison between them. The direction and polarization dependence of spectra are also measured.

[a)]Electronic mail: yugami@cc.mech.tohoku.ac.jp

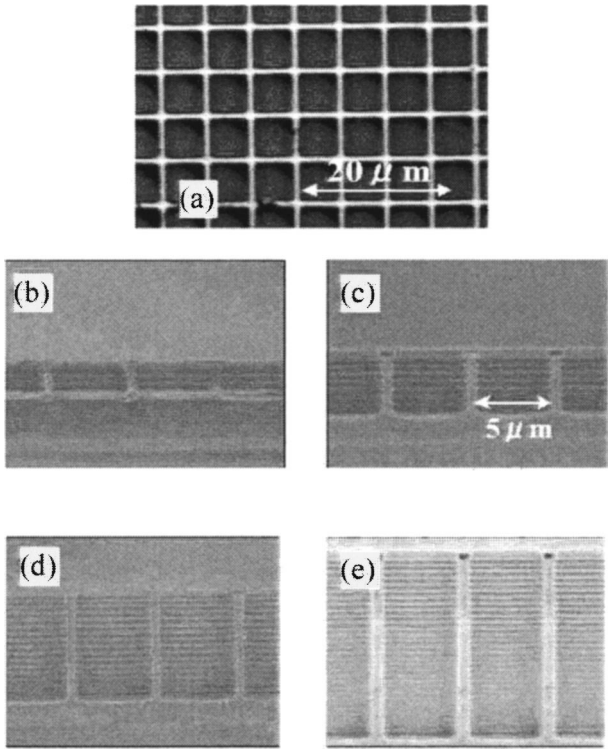

FIG. 1. The top, (a) and cross sectional view of samples with $L_z = 2.0\ \mu$m, (b), 4.9 μm, (c), 7.3 μm, (d), and 13.7 μm (e) are shown. SEM images from (b) to (e) are taken by the same magnifications.

The normal spectral emittance of the samples heated in a vacuum is shown in Fig. 2. Comparing the emittance of a flat sample, a very clear fine structure as well as emittance enhancement is obtained for all samples. The emittance peak intensity increases with an increasing depth of the microcavity, i.e., the aspect ratio of cavity. The six times enhancement of the emittance is obtained for sample IV. It is also found that the peak position and relative intensity of the emittance drastically changed with a change in the depth of microcavity. The enhancement of the emittance is observed only below the 10 μm region. This result is consistent with the model of CQE,[9] where the cut off wavelength, λ_c is expected to be 10 μm ($=2L_x$) for deep cavity samples. These features of the spectra strongly suggest that the enhancement of the emittance can be attributed to the CQE. Two parts of the surface of the samples contribute to the emission spectra shown in Fig. 2. One is the emission from microcavity and the other is the top flat surface of cavity walls. Assuming that the radiation intensity is in proportion to the area of these two parts, the emittance of microcavity; ϵ_c is estimated from the following equation,

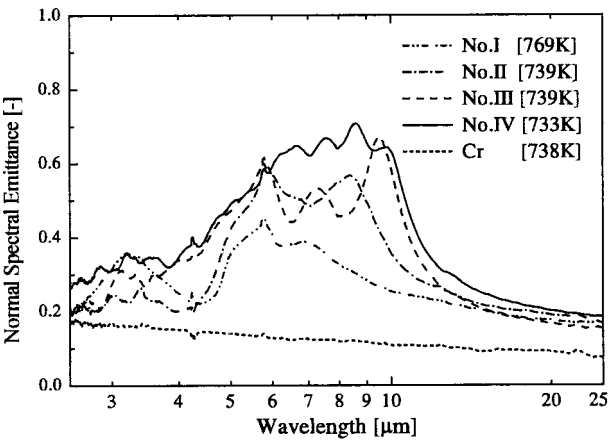

FIG. 2. Normal spectral emittance of microstructured samples is shown. The data of a sample with a Cr coated flat surface is also presented for comparison. The measured temperature is shown.

$$\epsilon_c = \frac{1}{A_c}(A_t\epsilon_t - A_s\epsilon_s), \tag{1}$$

where A_c is the area of aperture of a microcavity, A_s is the area of the top side of the walls, and $A_t = A_c + A_s$. ϵ_t and ϵ_s are the measured emittance of microstructured and flat samples, respectively. In this experiment, A_c and A_s are fixed to 25 and 11 μm^2. Using these values and Eq. (1), the value of ϵ_c at the highest peak position is estimated to be more than 0.9 for samples III and IV. This result reveals that the microcavity with an aspect ratio of 1.5 to 2 behaves as a quasiblackbody radiator, and the high-density microcavity structure at the surface is important for bringing out the effect of the microcavity.

It should be also pointed out in Fig. 2 that the baseline emittance of microcavity array samples is higher than that of flat samples at a long wavelength region ($\lambda > \lambda_c$). This cannot be explained by the CQE model, where the emission intensity at $\lambda > \lambda_c$ region should be supressed by the cavity effect. Taking this result into account, the low emissivity of the base material is very important to obtain the clear selective emission bands.

The direction and polarization dependence on the spectral emittance of sample III is shown in Figs. 3(a) and 3(b), respectively. The peak position of dominant peaks shows very little directional dependence within the measured range. However, the spectral shapes seem to be changed by changing the observed direction at the wavelength range between 3 to 6 μm. This spectral change may be attributed to the effect of spatial correlation between cavities with the repeat distance 6 μm. The directional dependence of the spectral emittance at the region of $\lambda > \lambda_c$ may be attributed to the influence of the emission from the smooth surface on the edge.

It is clearly demonstrated in Fig. 3(b) that the thermal radiation from two-dimensional cavity arrays has a random polarization nature. This is very different from the experimental results on the one-dimensional microgroove. In that case, the strong polarization dependence of thermal emission has been observed.[3]

As a preliminary analysis, we have compared the peak position of the observed emission bands with the discrete electromagnetic modes predicted by a simple theory of the cavity resonator. We have used the following boundary conditions; (1) the transverse electric field is zero on the cavity walls, and (2) the free and condition is applied at the aperture end of the cavity. Under these conditions, the electromagnetic modes (Λ) exist in the cavity is expressed by

$$\Lambda = \frac{2}{\sqrt{\left(\frac{1}{L_x}\right)^2 + \left(\frac{m}{L_y}\right)^2 + \left(\frac{2n+1}{2L_x}\right)^2}}, \tag{2}$$

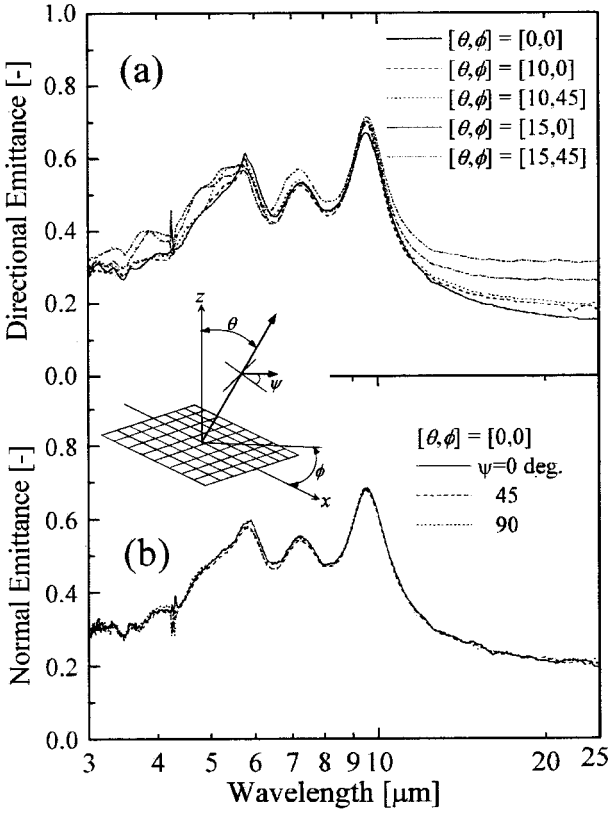

FIG. 3. The direction and polarization dependence of spectral emittance measured on sample III are shown. The coordination of angles is shown in the inset. The numbers in brackets represent the angles in degrees.

where *l*, *m*, and *n* are positive integers. According to Eq. (2), the maximum wavelength of Λ, which corresponds to the cut off frequency λ_c, is predicted to be $2L_x$ for deep cavity samples. The positions of electromagnetic modes calculated from Eq. (2) with various sets of integers are shown in Fig. 4 by vertical lines together with the spectrum of sample III. The calculated result shows good agreement with the dominant emittance peak at the longer wavelength region. However, the relationship between the observed structure in the spectrum and the calculated modes is not clear within this simple model. The more detailed analysis using coupled wave analysis will be published in subsequent letters.

In conclusion, we have clearly demonstrated the discrete thermal emission peaks from a two-dimensional cavity array. It is found that the aspect ratio from 1.5 to 2.0 is enough to obtain the high spectral-emitance intensity at the selective region. The low-emittance property of the base material is essential to obtain the highly selective emission phenomena. The directional and polarized emission spectra measurements reveal that the thermal emission from a two-dimensional microcavity shows isotropic and random polarization characters. The wavelengths of electromagnetic modes calculated by the cavity resonator model show good agreement with the dominant peaks of spectra. This study shows that the surface microcavity structure made on low-emissivity material surface is very efficient to control of thermal radiation.

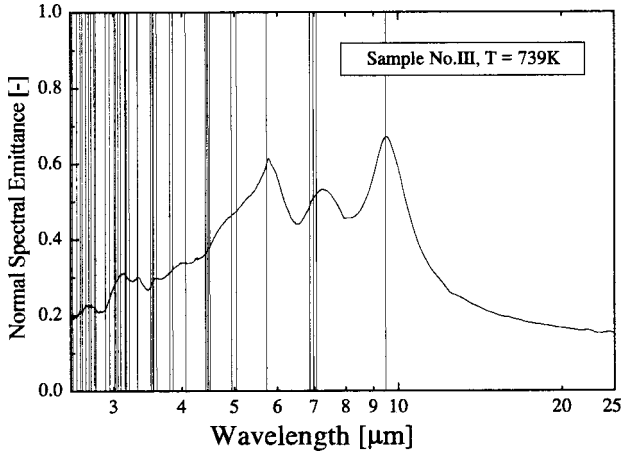

FIG. 4. Comparison between spectral emittance and the calculated cavity modes for sample III is shown.

The authors are greatly indebted to all of the people of the Venture Business Laboratory in Tohoku University for making the samples.

[1] M. Perlmutter, J. R. Howell, Trans. ASME J. Heat Transfer **85**, 282 (1963).
[2] S. Maruyama, Trans. Jpn. Soc. Mech. Eng., Ser. B **57**, 1084 (1991).
[3] P. J. Hesketh, J. N. Zemel, and B. Gebhart, Nature (London) **324**, 549 (1986).
[4] P. J. Hesketh, B. Gebhart, J. N. Zemel, Trans. ASME J. Heat Transfer **110**, 680 (1988).
[5] T. K. Wang and J. N. Zemel, Appl. Opt. **31**, 732 (1992).
[6] A. Heinzel, V. Boerner, A. Gombert, V. Wittwer, and J. Luther, AIP Conf. Proc. **460**, 191 (1999).
[7] H. Sai, H. Yugami, Y. Akiyama, Y. Kanamori, and K. Hane, J. Opt. Soc. Am. A **18**, 1471 (2001).
[8] J. F. Waymouth, J. Light Visual Environ. **13**, 51 (1989).
[9] S. Haroche and D. Kleppner, Phys. Today **42**, 24 (1989).